

Multiplexing of radio-frequency single-electron transistors

T. R. Stevenson,^{a)} F. A. Pellerano, and C. M. Stahle
NASA Goddard Space Flight Center, Codes 553 and 555, Greenbelt, Maryland 20771

K. Aidala and R. J. Schoelkopf
Department of Applied Physics, Yale University, P.O. Box 208284, New Haven, Connecticut 06520-8284

(Received 26 July 2001; accepted for publication 1 March 2002)

We present results on wavelength division multiplexing of radio-frequency single-electron transistors. We use a network of resonant impedance matching circuits to direct applied rf carrier waves to different transistors depending on carrier frequency. A two-channel demonstration of this concept using discrete components successfully reconstructed input signals with small levels of crosscoupling. A lithographic version of the rf circuits had measured parameters in agreement with electromagnetic modeling, with reduced crosscapacitance and inductance, and should allow 20–50 channels to be multiplexed. © 2002 American Institute of Physics. [DOI: 10.1063/1.1472472]

Several types of superconducting photodetectors are being developed for astronomical applications.^{1–3} Despite the complexity of cryogenic operation, such detectors are desirable because of capabilities such as single-photon spectroscopy, or extreme levels of sensitivity, which cannot be obtained with uncooled detectors. Large format arrays will require integration of the detectors with sensitive, fast, compact, low-power, multiplexable, on-chip amplifiers. Multiplexing schemes⁴ have been developed for low impedance detectors¹ with dc superconducting quantum interference device (SQUID) readout amplifiers. For high impedance detectors,^{2,3} the radio-frequency single-electron transistor (rf-SET)⁵ seems well suited as a readout amplifier.⁶ In this letter, we describe experimental demonstrations and theoretical limits of a wavelength division multiplexing (WDM) scheme⁶ in which a network of resonant circuits sorts and directs rf power, simultaneously applied at many carrier frequencies, to individually power and probe a collection of rf-SET amplifiers using a single rf following amplifier.

SETs are cryogenic quantum-effect devices which utilize quantization of charge on a small conducting island to yield a very high performance electrometer.⁷ A SET amplifier dissipates only picowatts of power and has subfemtofarad input capacitance. With a rf readout technique, the rf-SET increases the readout bandwidth of the SET greatly, to over 100 MHz, by using a resonant LC circuit to better match the ≈ 100 k Ω output impedance of the SET to a following amplifier.

To multiplex rf-SETs, we use a scheme similar to one used for rf-SQUIDs.⁸ We connect the following amplifier via a coaxial line to a parallel combination of LC circuits, one for each SET [see Fig. 1(a)]. As for a single rf-SET, a directional coupler is used to apply rf carrier power to the LC circuits while monitoring reflected power with a cryogenic high electron mobility transistor (HEMT) amplifier. Each LC circuit has a unique resonance frequency, and instead of a single frequency carrier wave, a frequency comb is generated with a component for each resonance. Gate signals modify SET output impedances, and the variation of the reflected

power signal at each carrier frequency can be decoded and demodulated with room temperature rf electronics. Simultaneous readout of all channels is possible.

Efficient coupling of carrier power to the i th SET, and sensitive detection of its reflected power signal, depend on transforming that SET's output impedance R_i downward to a value close to the $R_c = 50 \Omega$ input and noise impedance of the HEMT amplifier. The L-section circuit⁹ consisting of C_{1i} in parallel, and L_{1i} in series, with R_i transforms R_i to an effective resistance $r_i = R_i/Q_T^2$ at point A in Fig. 1(a), where $Q_T^{-1} = (L_{1i}/C_{1i})^{1/2}/R_i$ is the fractional bandwidth over which the transformation is effective around the resonance frequency $\omega_{1i} = [(1 - Q_T^{-2})/(L_{1i}C_{1i})]^{1/2}$. If the SETs are biased to a common value of $R_i = R_s$, then the desired impedance transformation requires a common bandwidth $Q_T^{-1} = (R_c/R_s)^{1/2}$ and ratio $L_{1i}/C_{1i} = R_c R_s$ for all channels. Multiple circuits can be paralleled with modest interaction since, at a given carrier frequency, one circuit is nearly a

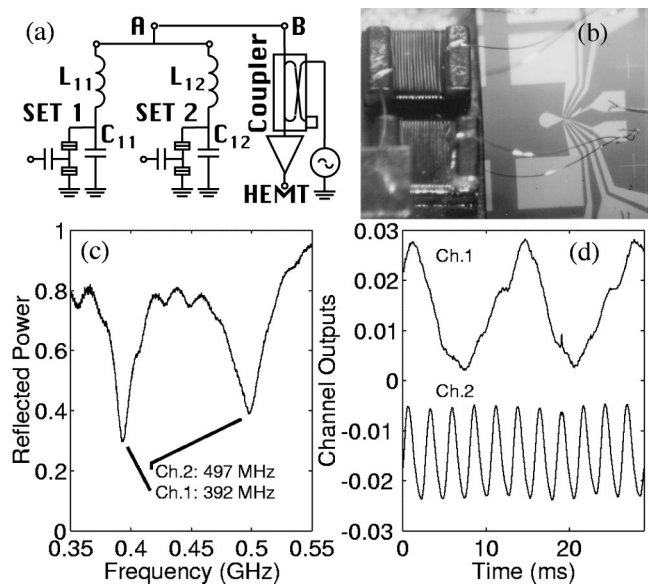


FIG. 1. (a) Circuit for wavelength division multiplexing of rf-SETs. (b) Two-channel demonstration using wire coils bonded to pads on SET chip. (c) Frequency dependence of reflected power ratio with SETs in high/low impedance states. (d) Demultiplexed SET signals.

^{a)}Electronic mail: thomass@pop500.gsfc.nasa.gov

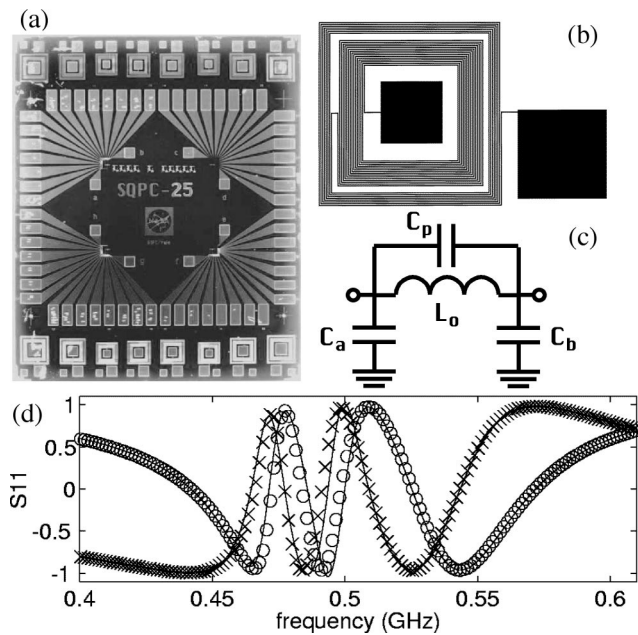


FIG. 2. (a) Lithographic rf circuits: 16 inductors of 5 designs are at top and bottom; 68 bonding pads connecting to 4 electron-beam fields serve as capacitors C_{1i} . (b) Geometry to minimize cross coupling (smallest coil, 619 μm outer side). (c) Parametric inductor model. (d) Real (o) and imaginary (x) parts of measured s -parameter for three circuit array, and fitted model curves (solid lines).

short circuit, while its nonresonant neighbors have large reactances.

To investigate this rf multiplexing scheme using two channels, we wirebonded two chip inductors¹⁰ to a pair of SETs on one silicon chip [see Fig. 1(b)]. The other ends of the inductors were bonded to a SMA microstrip launcher and coax leading from the 250 mK sample stage on a ³He refrigerator to a directional coupler and HEMT amplifier¹¹ at 4 K. Inductances were near 200 nH, and the ≈ 0.5 pF tank capacitance consisted of pad capacitances to ground.

The rf power reflected from the parallel combination of the two tank circuits is shown versus frequency in Fig. 1(c). The two resonance frequencies were 392 and 497 MHz. Figure 1(d) shows in the time domain the demultiplexed outputs of the two rf-SETs responding to different gate triangle-wave signals. The open-loop response to the ramping gate signals was approximately sinusoidal for each rf-SET. With Fourier analysis of the Fig. 1(d) data, we found an 8% coupling of Ch. 2 in the Ch. 1 output, and 4% of Ch. 1 in Ch. 2. This cross-coupling effect, where impedance changes of one SET off-resonance perturb the reflection of the carrier allocated for a different SET, will be diminished when feedback is used to fix each SETs operating point. The closed-loop coupling will then depend on the crosscapacitance between gates, which we can reduce by adding appropriate grounded guard traces.

Producing arrays of tank circuits by hand selection and assembly of discrete components clearly has limitations. We next made tank circuits patterned by optical lithography directly on substrate chips designed for SET fabrication by electron-beam lithography [see Fig. 2(a)]. We used planar three-dimensional electromagnetic modeling software¹² to design our circuit elements to minimize unwanted crossinductance and capacitance, and to give desired resonance fre-

quencies and impedance transforming properties. Figure 2(b) shows the coil geometry, with N_0 outer turns and $2N_0$ counter-wound inner turns of equal total areas, which we chose to reduce mutual inductance between nearby coils to $<1\%$. The coil is a type of second order gradiometer, and self-fields decay rapidly outside the gap separating inner and outer windings. On 550- μm -thick silicon chips, we fabricated 6 μm pitch coils of five sizes from superconducting niobium to reduce dissipation. With wire bonds, we connected the inner coil pads to tapered gold traces leading to electron-beam writing fields. Since internal self-resonance frequencies of the coils were designed to be above 1 GHz, we found we could accurately describe the results of our numerical modeling of one tank circuit by the lumped element model in Fig. 2(c). The coil sizes ranged from 619 to 803 μm . The calculated parameters L_0 and C_p shown in Fig. 2(c) ranged from 151 to 254 nH and 77 to 94 fF. The capacitance C_b on the coax side was about 200 fF, while the capacitance $C_a = C_{1i}$ on the SET side was about 75 fF from coil windings, 50 fF from inner coil pad, and 375 fF from the gold trace, for 500 fF total. We calculated the gold trace capacitance consisted of 0.2 pF directly to ground and 0.1 pF to each of its nearest neighbors. However, we normally used only every second trace, with intervening traces grounded, in which case the calculated cross capacitance was ≈ 10 fF. The resonance frequencies 393, 441, 476, 509, and 556 MHz were designed to span the band of our HEMT.

To test our rf modeling, we made calibrated s -parameter measurements of the reflection coefficient of various unloaded tank circuit arrays with coils in the superconducting state at 4 K. Figure 2(d) shows results for the three middle-sized circuits in parallel. The measured resonance frequencies of 465, 494, and 543 MHz were about 5% higher than designed. The lowest internal resonance frequencies for those inductors were 1036, 1121, and 1236 MHz—all above 1 GHz as expected. The circuits were lossless to the measurement precision, with Q values >500 . While it was not possible to extract the individual model parameters, when we fitted to expected functional forms we found measurable combinations of capacitances or inductances were within $\approx 10\%$ of our modeling results. By considering the relative spacing of poles and zeros, we tested for the presence of crosscapacitance between C_{1i} and estimated that actual crosscapacitance was $\approx 2\%$ or less, consistent with our calculation of 10 fF out of 500 fF with grounded traces between each tank circuit. When we used two adjacent gold traces for neighboring circuits, we observed splitting of the strongly coupled modes by $\approx \pm 50$ MHz, in agreement with calculations.

The lithographic circuits we successfully designed and tested have $(L_{1i}/C_{1i})^{1/2} \approx 670 \Omega$, implying they will somewhat overtransform a typical $R_s \approx 50 \text{ k}\Omega$ to $r_i = 9 \Omega$ instead of 50 Ω , with a factor of 2 degradation in power coupling to the SET, from 100% to 50%. We did this to increase the number of channels we can multiplex within the octave bandwidth (300–600 MHz) of our HEMT amplifier. We calculate a reasonably small level of open-loop coupling (nulled in closed-loop) exists between rf channels separated by at least $\Delta\omega = 2\omega_{1i}/Q_T$. That limits the maximum number of channels to $N \approx Q_T/3$ in an octave bandwidth, giving N

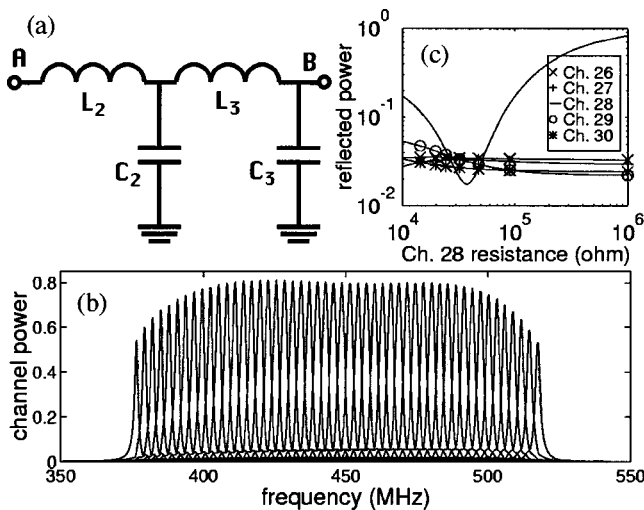


FIG. 3. (a) Two-stage impedance up-converter to add between points A and B in circuit of Fig. 1(a). (b) Power dissipated in each of 50 channels in a design with $50\text{ k}\Omega$ transformed down to $0.5\ \Omega$, then up to $50\ \Omega$. (c) Typical example of power changes measured at adjacent carrier frequencies when output of one SET (e.g., $i=28$) varies.

≈ 25 instead of 11 when transforming to $9\ \Omega$ instead of $50\ \Omega$.

One option to increase N without sacrificing coupling is to overtransform, but then to insert a single impedance up-transforming circuit [see Fig. 3(a)] between points A and B in Fig. 1(a). Figure 3(a) shows a two-stage circuit, but a single stage with just L_2 and C_2 could be used. In that case, the fractional widths of the transformations of R_s down to some value r_a and then up to R_c are, respectively, $Q_T^{-1} = (r_a/R_s)^{1/2}$ and $Q_2^{-1} = (r_a/R_c)^{1/2}$, which allows $N = Q_T/Q_2/2 = (R_s/R_c)^{1/2}/2$, or $N=16$ for a $R_s=50\text{ k}\Omega$ to $r_i=50\ \Omega$ overall transformation. With a single stage, N is independent of r_a , but the fixed number of channels can in theory be packed into any desired following amplifier bandwidth. However, with two stages, up-transformation bandwidth can be increased to $Q_2^{-1} = Q_3^{-1} = (r_a/R_c)^{1/4}$, with $N = R_s^{1/2}/(r_a R_c)^{1/4}/2$ increasing for decreasing r_a .

Choosing two stages and $r_a=0.5\ \Omega$ to get $N=50$, we find components which we believe we can fabricate with acceptable parasitic values based on our electromagnetic modeling and fabrication results: $L_{1i}=73\text{--}53\text{ nH}$, $L_2=0.55\text{ nH}$; $L_3=5.7\text{ nH}$, $C_{1i}=2.5\text{--}1.8\text{ pF}$, $C_2=218\text{ pF}$, and $C_3=23\text{ pF}$. Coil dimensions are less than $500\ \mu\text{m}$ on a side. Figure 3(b) shows the predicted frequency dependence of the power dissipated, relative to the maximum extractable from the source, in each SET with $R_i=R_s=50\text{ k}\Omega$. Crosscoupling between reflected power signals measured at consecutive carrier frequencies is shown in Fig. 3(c). As one SET resistance is increased from R_s , the reflected power for its chan-

nel increases rapidly while nearby channels are relatively unaffected. The ratio of differential sensitivities is $\approx 10\%$ at $R_i=R_s$, but decreases to 1% or less at $R_i=2R_s$.

In conclusion, we have demonstrated the ability to both supply power to and multiplex outputs of many SETs using only a single rf connection. Our technique exploits the ability of a network of resonant impedance matching circuits to direct applied carrier waves to different SETs depending on frequency. Unlike time division, our WDM method allows simultaneous readings on all channels, with no potential loss of signal-to-noise ratio. The maximum number of channels is limited only by practicality of fabricating appropriate components. Using optical lithography and electromagnetic modeling, we were able to fabricate superconducting circuits capable of multiplexing about 20–50 channels. Such a system would provide a compact on-chip readout for arrays of superconducting photon detectors.

The authors thank Peter Wahlgren, Abdelhanin Aassime, and Per Delsing of Chalmers University for SET fabrication, and Richard Bradley for supplying our HEMT amplifier. This work was supported by internal GSFC Director's discretionary funds, and the NASA Explorer and Cross Enterprise Technology Development programs.

- ¹R. W. Romani, R. W. Miller, B. Cabrera, E. Figueroa-Feliciano, and S. W. Nam, *Astron. J.* **521**, L153 (1999); K. D. Irwin, G. C. Hilton, J. M. Martinis, S. Deiker, N. Bergren, S. W. Nam, D. A. Rudman, and D. A. Wollman, *Nucl. Instrum. Methods Phys. Res. A* **444**, 184 (2000); N. Tralshwala, R. P. Brekosky, M. J. Li, E. Figueroa-Feliciano, F. M. Finkbeiner, M. A. Lindeman, C. M. Stahle, and C. K. Stahle, *IEEE Trans. Appl. Supercond.* **11**, 755 (2001).
- ²A. Peacock, P. Verhoeve, N. Rando, A. van Dordrecht, B. G. Taylor, C. Erd, M. A. C. Perryman, R. Venn, J. Howlett, D. J. Goldie, J. Lumley, and M. Wallis, *Nature (London)* **381**, 135 (1996).
- ³R. J. Schoelkopf, S. H. Moseley, C. M. Stahle, P. Wahlgren, and P. Delsing, *IEEE Trans. Appl. Supercond.* **9**, 2935 (1999).
- ⁴J. A. Chervenak, E. N. Grossman, K. D. Irwin, J. M. Martinis, C. D. Reintsema, C. A. Allen, D. I. Bergman, S. H. Moseley, and R. Shafer, *Nucl. Instrum. Methods Phys. Res. A* **444**, 107 (2000); J. Yoon, J. Clarke, J. M. Gildemeister, A. T. Lee, M. J. Meyers, P. L. Richards, and J. T. Skidmore, *Appl. Phys. Lett.* **78**, 371 (2001).
- ⁵R. J. Schoelkopf, P. Wahlgren, A. A. Kozhevnikov, P. Delsing, and D. E. Prober, *Science* **280**, 1238 (1998).
- ⁶T. R. Stevenson, A. Aassime, P. Delsing, R. Schoelkopf, K. Segall, and C. M. Stahle, *IEEE Trans. Appl. Supercond.* **11**, 692 (2001).
- ⁷T. A. Fulton and G. J. Dolan, *Phys. Rev. Lett.* **59**, 109 (1987).
- ⁸M. Muck, *IEEE Trans. Magn.* **27**, 2986 (1991).
- ⁹L. Weinberg, *Network Analysis and Synthesis* (McGraw-Hill, New York, 1962).
- ¹⁰Part No. 0805CS-221XKBC, Coilcraft, 1102 Silver Lake Road, Cary, IL 60013.
- ¹¹Our HEMT amplifier was provided by the National Radio Astronomy Observatory, 2015 Ivy Road, Suite 219, Charlottesville, VA 22903.
- ¹²SONNET®, Sonnet Software, Inc. 1020 Seventh North St., Suite 210, Liverpool, NY 13088.